Acta Crystallographica Section D
Biological Crystallography
ISSN 0907-4449

Strongly correlated structure of axial-symmetric proteins. I. Orthorhombic, tetragonal, trigonal and hexagonal symmetries

A. Janner

Institute for Theoretical Physics, Radboud University, Toernooiveld, 6525 ED Nijmegen, The Netherlands

Correspondence e-mail: alo@sci.kun.nl

Received 23 March 2004
Accepted 9 December 2004

The geometry of the molecular envelope and channel in axial-symmetric proteins is investigated in order to test the validity of rules deduced previously from several other biomacromolecules. Again, molecular forms with remarkable geometric properties are found. In particular, for order of rotation $N = 2$, 3, 4, 6 the molecular forms encapsulating the C^{α} backbone of the protein have vertices at lattice points and therefore integral indices. These lattices are characterized by a height-to-width axial ratio that reduces the number of free parameters and enhances the symmetry.

1. Introduction

Previous investigations of the geometry of proteins with axial point-group symmetry (Janner, 2001, 2002*a*,*b*,*c*, 2003*a*,*b*,*c*) have revealed unexpected geometrical properties of their molecular envelope and of the central channel in the C^{α}-backbone description.

In this series of articles, 19 additional axial-symmetric proteins have been investigated in order to verify the generic character of the geometrical features observed: eight in part I (this work), six in part II (Janner, 2005*a*) and five in complex with DNA/RNA in part III (Janner, 2005*b*). The molecular forms considered delimit the given molecule by planes which, in a first approximation, are taken parallel and perpendicular to the rotational axis. Their intersection defines a prism with two basal and a number of lateral faces. A refinement then yields, in general, polyhedral molecular forms which have the following remarkable geometric properties: vertices at points of a lattice, which has a characteristic axial ratio c/a, and crystallographic scaling relating the central hole to the external envelope. Some of these properties recall those of crystal-growth forms; others are new, even if also present in particular crystal cases, as shown later. In the next section, these basic properties are outlined in the two-dimensional description obtained by projecting the structures in the direction parallel or perpendicular to the rotational axis.

2. Crystallographic confinement of polypeptide chains

The crystallographic properties mentioned above apply to the molecular forms confining the polypeptide chains of axial-symmetric proteins and not to the chains themselves. Of course, form and content are related to each other: in particular, when a chain reaches the boundary it has either to stop or to fold. This aspect has been discussed in detail in previous publications on the chaperonin complex GroEL–GroES (Janner, 2003*a*,*b*,*c*). In this survey, it is only mentioned occasionally, with an analysis of possible consequences given at the end of part II.

2.1. Form lattice and Law of Rational Indices

All the molecular forms investigated obey the same Law of Rational Indices as in growth forms of crystals. This implies the possibility of assigning sets of rational integers (the indices) to vertices and to facets. In crystals only the facets are indexed because of the growth. In the molecular case, it is convenient to index the vertices. In both cases, the delimiting planes are lattice planes. In proteins it is fully unexpected to find an underlying lattice structure, because there are no lattice translations in a molecule. Therefore, it is necessary to distinguish carefully between the crystal lattice and the form lattice, as they are different.

A form lattice is a lattice of a polyhedral form having vertices at lattice points.

The form lattice does not represent translational symmetry and has a distinctive origin, which is the centre of the point-group rotations of the form (and of the enclosed structure). A typical example of a two-dimensional form lattice can be seen in a snow crystal, where, as in in the proteins considered, the form has external and internal boundaries obeying the Law of Rational Indices mentioned above (Fig. 1). This is a general property of snowflakes and many more examples have been reported elsewhere (Janner, 2002*d*).

The molecular form of R-phycoerythrin in a projected view along the threefold axis is also hexagonal and very similar (Fig. 2). The radius r_e of the envelope is four times that of the central channel r_0, which defines the a parameter of the form lattice, so that the vertices of the envelope have the same indices 40, 44, 04, $\bar{4}0$, $\bar{4}\bar{4}$ and $0\bar{4}$ as the snowflake in Fig. 1.

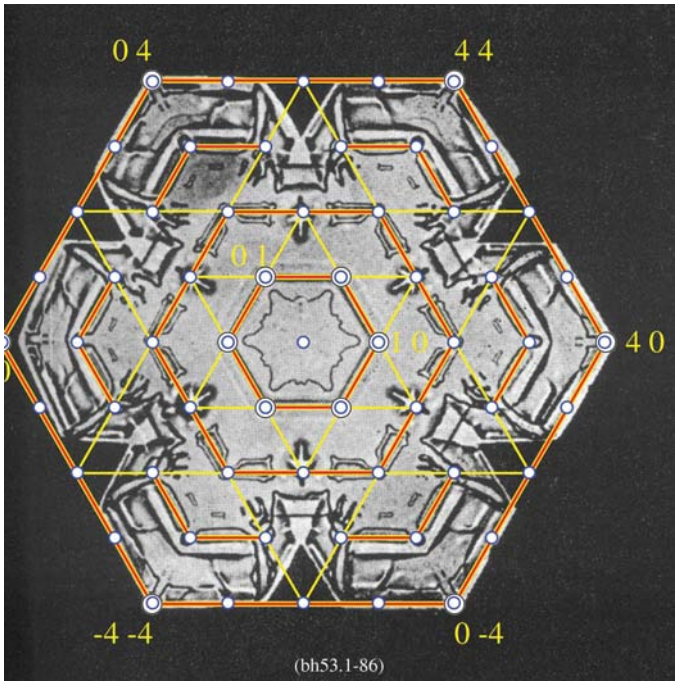

Figure 1
This snowflake, taken from Bentley & Humphreys (1931) (reproduced courtesy of Dover), has hexagonal patterns with vertices at points of a lattice, denoted as a form lattice. This allows the assignment of integral coordinates (indices) to these vertices. Hexagrams drawn from hexagonal mid-edges are also indicated.

The mitochondrial creatine kinase octamer is the third example. In a projected view along the fourfold axis, it shows a square central hole, but the external boundary is not a square. Nevertheless, it also has vertices with integral indices, as indicated in Fig. 3. To see this, one again starts from a square

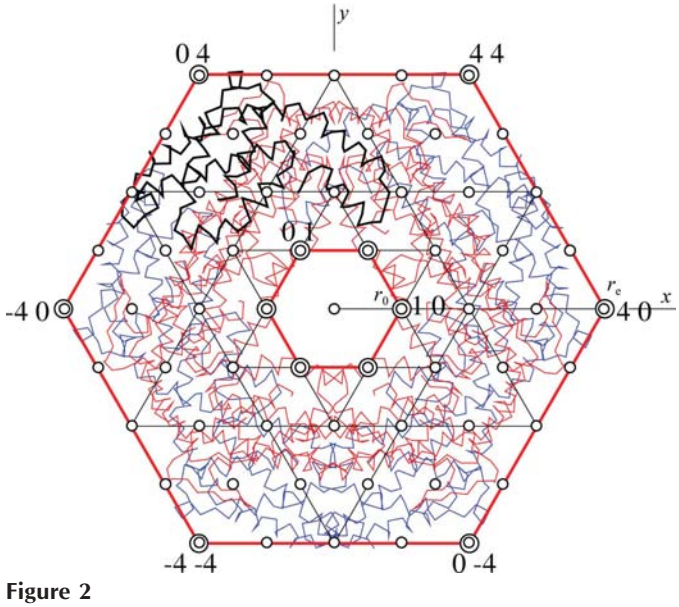

Figure 2
The hexameric R-phycoerythrin in a projected view along the threefold axis has the same hexagonal form as the snow crystal of Fig. 1. The radius r_e of the external envelope is four times the radius r_0 of the central hole, which fixes the lattice parameter $a = r_0$. In this figure and in the following figures a single monomer is enhanced by using a different linewidth.

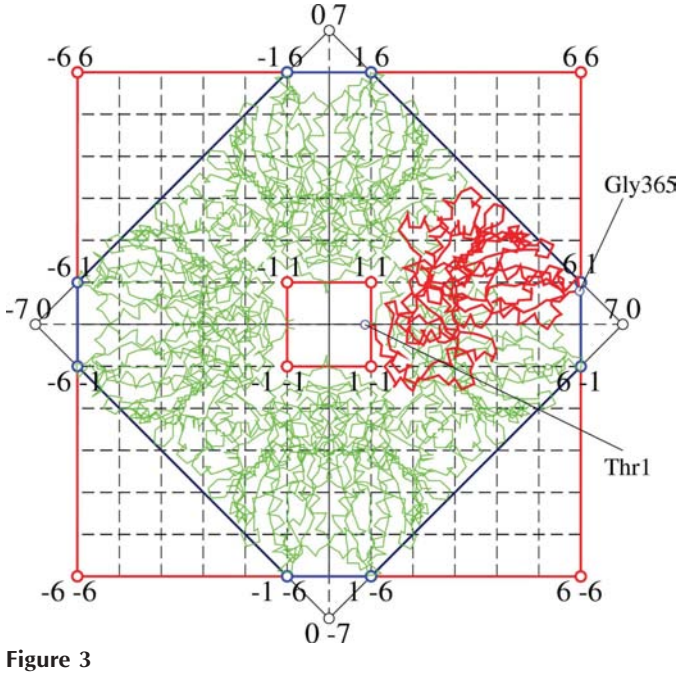

Figure 3
The mitochondrial creatine kinase octamer in a projected view along the fourfold axis has a square central hole which defines a square lattice, allowing the assignment of integral indices to the vertices of the molecular form. Successive approximations of the external envelope are shown. The two residues Thr1 and Gly365 indicated have an extremal radial distance from the fourfold axis and correspond to ideal positions at lattice points with indices 10 and 61, respectively.

lattice with parameter a given (approximately) by the shortest radial distance of the residue Thr1 at the beginning of each monomer. A sixfold larger square encapsulates the whole. It represents a first enclosing form with vertices at ±6 ±6. A better square envelope is obtained by a square turned by 45° with respect to the square of the channel and with vertices at ±7 0 and 0 ±7. Finally, the refined polygonal form is the truncated square obtained as the intersection of the two previous squares. It can then be recognized that the projected positions of the residue Gly365 in the eight chains is situated near the form vertices with indices 61, 16, $\bar{1}6$, $\bar{6}1$, $\bar{6}\bar{1}$, $\bar{1}\bar{6}$, $1\bar{6}$ and $6\bar{1}$.

2.2. Characteristic ratios

The polyhedral form of a protein is three-dimensional and so is the form lattice if it occurs. Let us consider the two previous examples, beginning with the octameric creatine kinase. The polyhedral form is a truncated square prism with a total height $H = 8a$ (see §4.1 and Fig. 12). Accordingly, a cubic form lattice with lattice parameter a allows integral indices for all the vertices. The existence of a cubic lattice is remarkable for an octamer, but nothing special from a crystallographic point of view.

The situation is far more intriguing in the case of the hexameric R-phycoerythrin, where the hexagonal prism of the enclosing form has a total height $H = 4r_0$, with r_0 being the radius of the hexagonal central hole and $r_e = 4r_0$ being the radius of the envelope, as mentioned previously (see Fig. 2). This implies that the radius of the prism is equal to the height. The same is true for the hexagonal form lattice, which has lattice parameters $c = a$, corresponding to an axial ratio $c/a = 1$ (Fig. 4). This special metrical relation is more common in crystals than one would think, so that the corresponding lattices deserve the special name of hexagonal isometric. Indeed, the plot of the distribution of hexagonal crystal lattices, corresponding to about 12 000 entries in the Inorganic Crystal Structure Database (ICSD), as a function of the axial ratio c/a (in $\delta = 0.05$ intervals) reveals that the highest peak corresponds to the isometric hexagonal lattice (Fig. 5), as reported at the European Crystallographic Meeting ECM22 (de Gelder & Janner, 2004). It can be seen that more sharp peaks occur at other special ratios. The form lattices of axial-symmetric proteins show similar characteristic ratios that reduce the number of independent lattice parameters from two to one (in the examples given, this single parameter is the radius r_0 of the hole). These special metrical relations in fact correspond to integral lattices, which are characterized by a metric tensor with integral entries (Janner, 2004*a*). In the axial symmetric proteins presented in this work, integral lattices are so dominant that the proteins are ordered according to the axial ratios of their molecular forms.

2.3. Crystallographic scaling

The third remarkable property observed is a crystallographic scaling relation between envelope and central channel which depends on the point-group symmetry of the form (and of the protein as well). The considerations here are restricted to the planar case, which can be discussed in two dimensions, where a scaling transformation S can be characterized by a scaling factor λ (describing a dilatation or a contraction) and a rotational angle φ. S is crystallographic if it applies lattice

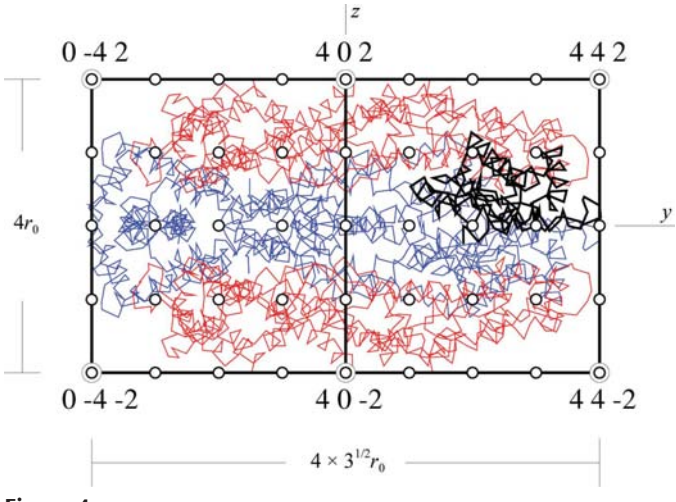

Figure 4
The hexameric R-phycoerithrin is shown projected along the x direction, perpendicular to the sixfold axis indicated in Fig. 2. The total height H of the form is $4r_0$ and is equal to the radius r_e of the hexagonal basal face. Accordingly, the corresponding form lattice has an axial ratio given by $c/a = 1$ and is hexagonal isometric. The lattice points are indicated by empty circles and the vertices of the enclosing form by double circles with corresponding integral indices.

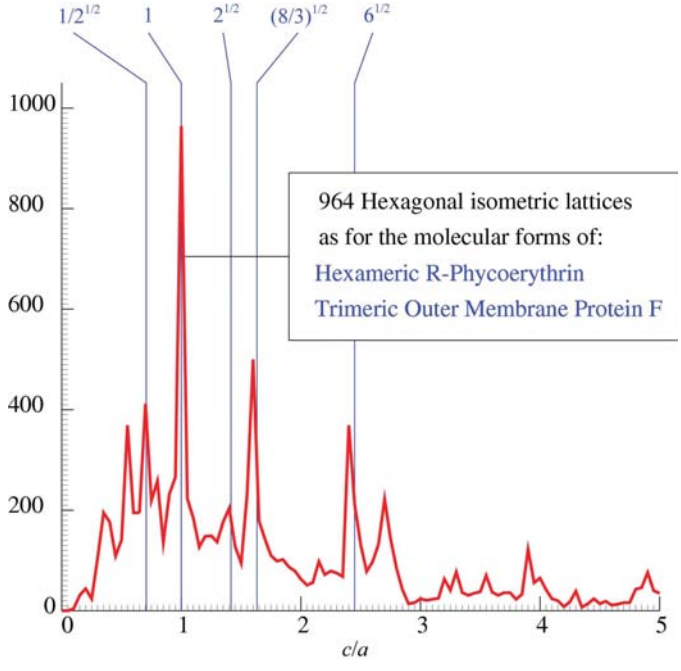

Figure 5
The number of crystals occurring in successive intervals $\delta = 0.05$ of the axial ratio c/a of their lattice form a distribution which shows sharp peaks approximatively at the special numerical values indicated, similar to those observed for the form lattices of the axial-symmetric proteins presented in this work. The highest peak occurs at the value $c/a = 1$, which corresponds to hexagonal isometric lattices.

points to lattice points. More precisely, a crystallographic scaling S transforms the unit cell of a form lattice Λ into one of a sublattice Σ with same point-group symmetry K,

$$S\,\Lambda = \Sigma, \quad \Sigma \subseteq \Lambda, \quad K\,\Lambda = \Lambda, \quad K\,\Sigma = \Sigma.$$

When expressed in a lattice basis of Λ, the transformation S is represented by an integral matrix. Its determinant is then λ^2. The inverse transformation S^{-1} has, in general, rational entries. Typical two-dimensional crystallographic transformations, which play a role in the projected views of the proteins discussed later, are given in Fig. 6. For the two hexagonal forms shown, the connection with star hexagons is outlined. The hexagrammal mid-edge relation occurs for $\lambda = 2$ and $\varphi = 0^\circ$ and the hexagrammal vertex scaling for $\lambda = 3^{1/2}$ and $\varphi = 30^\circ$ (Fig. 6). Similar polygrammal scaling relations play an important role in part II.

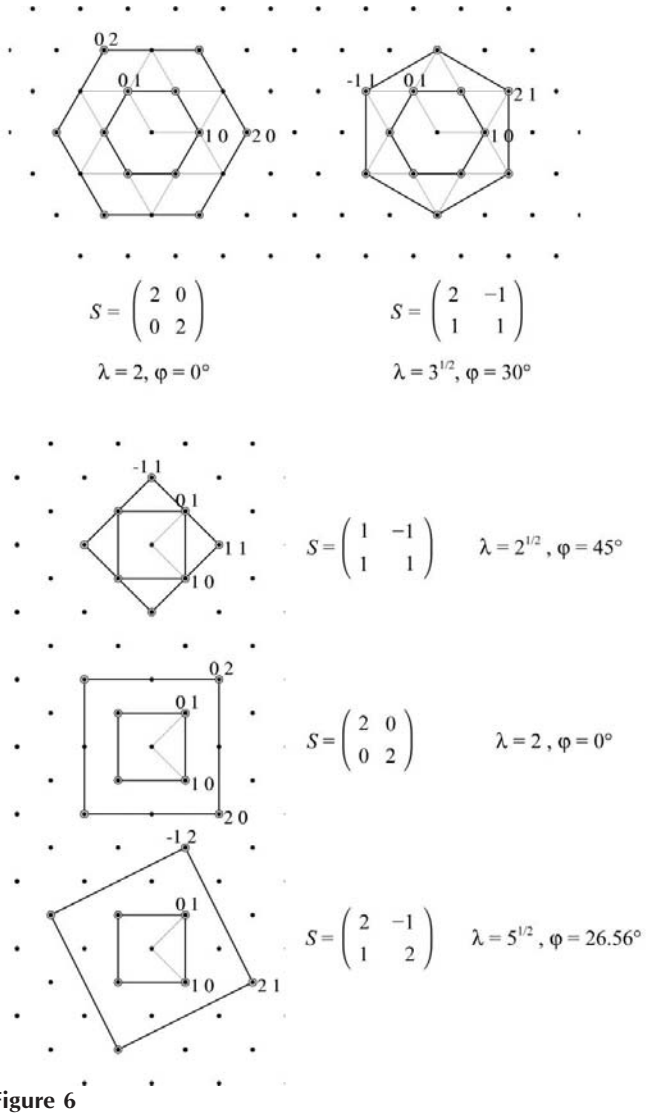

Figure 6
Two examples of hexagonal crystallographic scaling transformations are indicated by scaled forms (indexed), scaling matrix S, scaling factor λ and rotational angle φ, respectively. A similar representation is given for three examples with a square form lattice.

2.4. General considerations

In general, the point-group symmetry of the envelope and of the central channel is larger than that of the protein: 422 molecular forms are found for 222 proteins and 622 forms for a threefold protein; in part II, a decagonal channel is found while the symmetry of the protein is only pentagonal. The present work clearly indicates the generic validity (not necessarily a general validity) of the crystallographic confinement of axial-symmetric proteins. The deviations observed so far are mostly based on deviations from an ideal rotational symmetry of the chains involved or have a local character that is more pronounced at the chain ends. For a given axial symmetry, the C^α positions having an extremal radial distance from the axis in many cases determines the overall geometry of envelope and channel.

The obvious question about the mutual relation between the form lattice of a given protein and the lattice of the crystal in which the protein is embedded cannot yet be answered. The occurrence of non-crystallographic symmetries in crystals of biomacromolecules is an indication that if such a relation exists it is certainly not a trivial one.

In any case, the challenge remains to understand the crystallographic and physico-chemical nature of these remarkable geometric features and to derive the possible biological implications. The variety of the proteins involved and the relevance of integral lattices for a large number of crystals supports the idea that there is such a connection and that it is fairly general.

3. Proteins with trigonal and hexagonal symmetry

The following trigonal proteins are considered: R-phycoerythrin (R-PE; PDB code 1lia; Chang *et al.*, 1996), bacteriorhodopsin (bR; PDB codes 1qko and 1qhj; Edman *et al.*, 1999; Belrhali *et al.*, 1999), Pyr RNA-binding attenuation protein (PyrR; PDB code 1a4x; Tomchick *et al.*, 1998) and the porin outer membrane protein F (OmpF; PDB code 2omf; Cowan, 1993).

These proteins have either a hexagonal envelope and channel (R-PE and bR) or a trigonal channel and a trigonal/hexagonal envelope, depending on the approximation (PyrR and Ompf). In all these cases, the molecular form lattice is hexagonal with axial ratios c:a equal to 1 (the isometric case), $3^{1/2}$ or $2^{1/2}$.

3.1. Hexagonal isometric form lattice, c:a = 1

3.1.1. R-phycoerythrin (R-PE). The α and β subunits of R-phycoerythrin are assembled to form an $(\alpha\beta)_6$ hexamer with point-group symmetry 32 once the additional subunit γ is disregarded (as in the PDB file 1lia), despite the important role of γ in the light-harvesting process of this protein (Chang *et al.*, 1996). Both channel and envelope are hexagonal prisms, with bases scaled 1:4 in the two-step mid-edge hexagrammal relation (Janner, 2001) indicated in Fig. 6. Moreover, the height of the prism is equal to the radius r_e of the larger hexagon, as can be seen from the axial and perpendicular view

of R-PE (see Figs. 2 and 4). Accordingly, the molecular form lattice has an axial ratio $c{:}a = 1$ and one obtains $r_e = 4r_0 = 4a = 4c$, with r_0 the radius of the channel. The indices of the channel expressed with respect to the hexagonal lattice basis (a, a, c) and up to sixfold rotations around the z axis are 102, $10\bar{2}$ and those of the envelope are 402, $40\bar{2}$.

3.1.2. Porin outer membrane protein (OmpF). The biological unit of OmpF is a trimer (Cowan, 1993; PDB code 2omf) with point-group symmetry 3. It belongs to the family of bacterial porins (Cowan, 1993). As shown in Fig. 7, the channel is delimited by a triangular prism. The envelope, to a first approximation, is hexagonal. Despite this difference, both are in a hexagrammal scaling relation of the vertex type already mentioned (Janner, 2001).

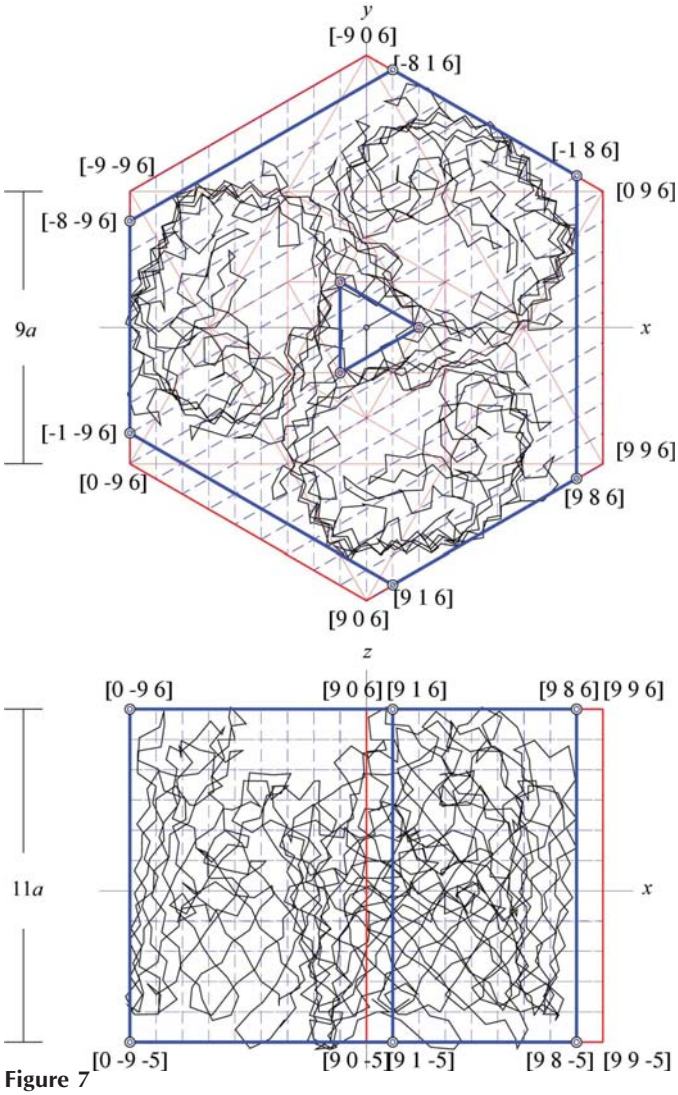

Figure 7
The trimeric outer membrane protein F (OmpF) has point-group symmetry 3. The channel is a triangular prism which is in a three-step hexagrammal scaling relation with the hexagonal envelope. The radius of the hexagon is $3 \times 3^{1/2}$ times the radius of the triangle. The planar indices 12, $\bar{2}\bar{1}$, $1\bar{1}$ of the hole are transformed by the scaling transformation S^3 (with an S matrix indicated in Fig. 6) into planar indices of the envelope $\bar{9}0$, $0\bar{9}$, 99, respectively. Only after having identified that the underlying molecular form lattice indicated by dashed lines is hexagonal isometric ($c{:}a = 1$) can it be recognized that the height, width and channel of OmpF are multiples of the parameter a.

Indeed, starting from the hexagonal vertices of the hole, by a three-step transformation which combines an expansion (in the xy plane) by a factor $3^{1/2}$ with an axial rotation of 30° (see Fig. 6), three coplanar vertices of the envelope are obtained. Accordingly, the radius of the resulting hexagon is $3^{1/2}$ times larger than the radius of the starting triangle and the planar indices 12, $\bar{2}\bar{1}$, $1\bar{1}$ of the channel are transformed by

$$S^3 = \begin{pmatrix} 2 & \bar{1} \\ 1 & 1 \end{pmatrix}^3 = \begin{pmatrix} 3 & \bar{6} \\ 6 & \bar{3} \end{pmatrix}$$

into planar indices of the envelope $\bar{9}0$, $0\bar{9}$, 99, respectively. Applying the scale-rotational transformation S^{-1} to the envelope four times, one obtains a (smaller) hexagonal channel scaled by a factor 9. The corresponding radius can be taken as the a parameter of the hexagonal molecular form

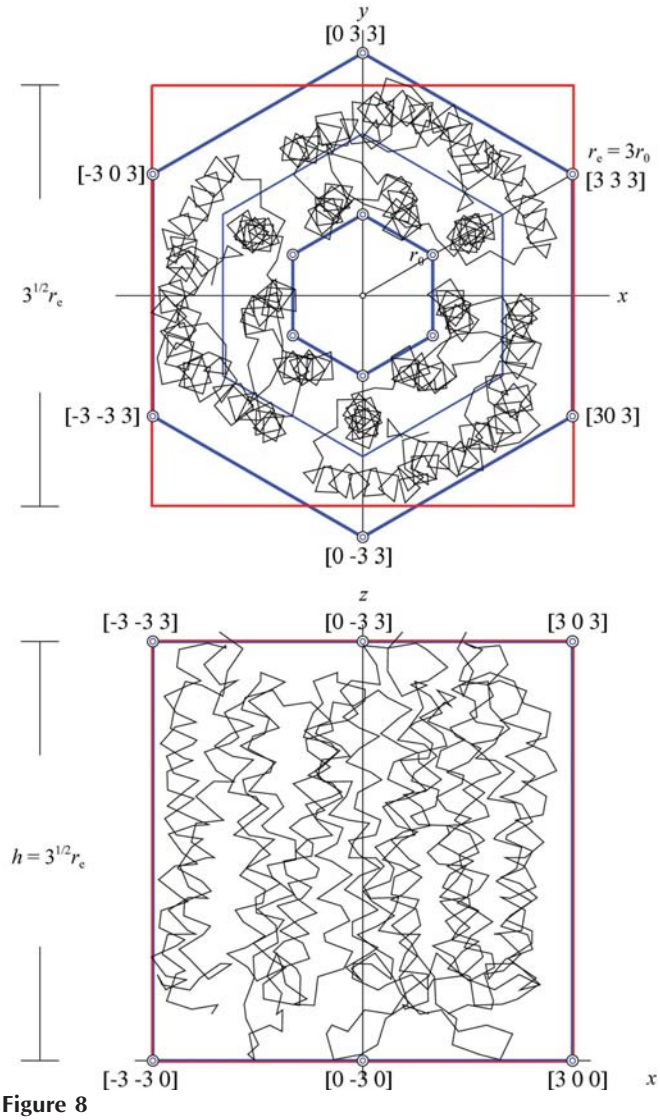

Figure 8
The bacteriorhodopsin trimer (bR) has a hexagonal envelope with a radius $r_e = 3r_0$, three times that of the channel. The height of the hexagonal prism is $3^{1/2}r_e$. Because of this special axial ratio, there is also a cubic envelope with edge length $3^{1/2}r_e$. This explains the compatibility of the trigonal OmpF with the cubic lipid phase used for the crystallization of this membrane protein.

lattice. It can then be verified that the height h of OmpF is a multiple of a and that with $h = 11c$ one arrives at the isometric ratio $c{:}a = 1$. This isometric hexagonal lattice allows a refined definition of the envelope with vertices indexed by 916, 986, $91\bar{5}$, $98\bar{5}$, together with the trigonal-related vertices. Corresponding vertices of the triangular channel are 126, $12\bar{5}$ and $\bar{2}1\bar{6}$, $\bar{2}1\bar{5}$, $1\bar{1}6$ and $1\bar{1}\bar{5}$ (see Fig. 7). A further refinement of the molecular form of OmpF reveals additional integral scale-rotational relations between the vertices. This may be interesting, but it is too detailed for the present aim.

3.2. Hexagonal form lattice with axial ratio $c{:}a = 3^{1/2}$

3.2.1. Bacteriorhodopsin (bR). Bacteriorhodopsin is a trimer which has been extensively studied in various configurations. Here, the structure of an early intermediate state of the photocycle is considered (Edman *et al.*, 1999; PDB code 1qko) instead of that of the ground state (Belrhali *et al.*, 1999; PDB code 1qhj) because it fits slightly better to the $3^{1/2}$ hexagonal case. In any case, the minor structural differences between the two states are not relevant from the morphological point of view. In bacteriorhodopsin, the channel and the envelope are related by similar hexagrammal scaling relations as in the previous OmpF protein. A two-step hexagrammal scale-rotational transformation of the vertex type now occurs, so that the channel is scaled by a factor of 3 from the hexagonal envelope (Fig. 8).

The axial ratio observed explains the compatibility of the bacteriorhodopsin trimer with the cubic lipid phase, used as crystallization medium for this membrane protein (Landau & Rosenbusch, 1996). Indeed, the height of the envelope is equal to its hexagonal width, so that the protein also fits in a cubic envelope with edge length $3^{1/2}r_e$, as indicated in Fig. 8. Taking for the hexagonal form lattice the parameter a equal to the radius r_0 of the channel and $c = 3^{1/2}a$, representative vertices of the channel with indices 100, 103 and 300, 303 are found for the envelope.

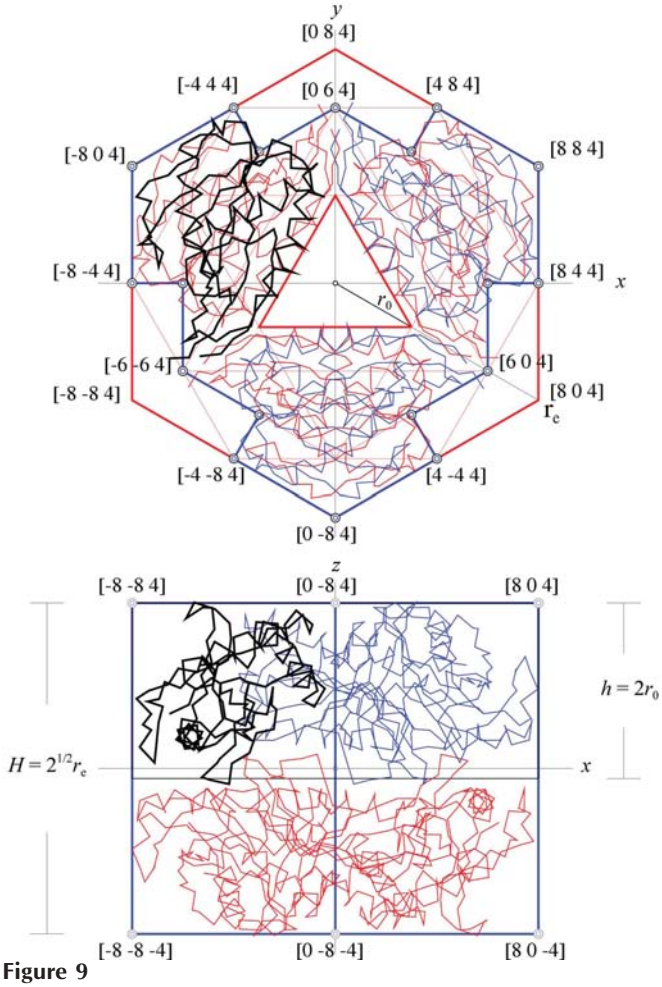

Figure 9
The point group of the hexameric Pyr RNA-binding attenuation protein (Pyr-R) has a triangular hole with radius r_0. The radius r_e of the hexagonal envelope, a factor 8/3 times larger, is related to r_0 by the outlined hexagrammal scaling. Both radii are in scaling relation with the height, which is $2^{1/2}r_e$ for the hexamer and $2r_0$ for the trimer. This implies that the corresponding molecular form lattices are integral with the same lattice parameter $a = r_0/3$ and axial ratios $2^{1/2}$ and 1, respectively.

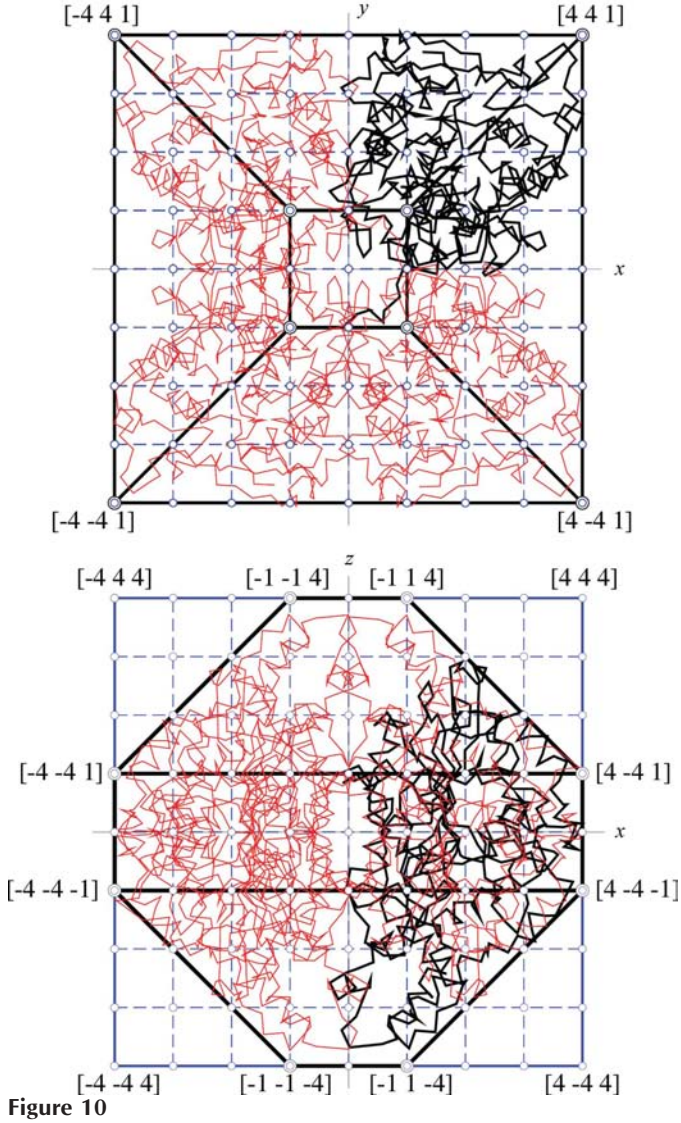

Figure 10
The *A. niger* acid phosphatase (AnigAP) is a tetramer with orthorhombic point-group symmetry. The envelope is a truncated square pyramid inscribed in a cube with edge length $8a$, where a is the parameter of a cubic lattice (indicated by dashed lines and empty circles).

3.3. Hexagonal form lattice with axial ratio $c{:}a = 2^{1/2}$

3.3.1. Pyr RNA-binding attenuation protein (PyrR). The point symmetry of the hexameric PyrR (Tomchick *et al.*, 1998; PDB code 1a4x) is 32. Its envelope is a combination of two hexagonal prisms, a larger one with radius r_e and a smaller one with radius $r'_e = 3r_e/4$. The triangular channel has a radius $r_0 = 3r_e/8$ (Fig. 9).

The value of the parameter a of the hexagonal molecular form lattice follows from this observation: $a = r_e/8 = r_0/3$. The height of the envelope of the hexamer is $H = 2^{1/2}r_e$. This leads to the value of the parameter c and to the corresponding axial ratio $c{:}a = 2^{1/2}$. Expressed with respect to the hexagonal basis (a, a, c), the indices of the vertices in the asymmetric unit of 32 are 304 for the channel and 604, 644, 844, 884, 484 and 364 for the envelope. Some of these coordinates can be seen in Fig. 9. Also interesting is the morphology of the PyrR trimer, which only differs in height with respect to the hexamer. One now has $h = 2r_0 = 6a$ (see Fig. 9). This implies an isometric axial ratio $c{:}a = 1$ for the trimer instead of the $c{:}a = 2^{1/2}$ ratio for the hexamer. The indices of the envelope and channel of the trimeric configuration only differ in the last index. Taking into account the asymmetric unit of point group 3, which is twice that of 32, the value 4 of third index of the set of vertices indicated above for the hexamer is replaced for the trimer by 6 and by 0, respectively.

4. Proteins with orthorhombic and tetragonal symmetry

This section includes the orthorhombic proteins *Aspergillus niger* acid phosphatase (AnigAP; PDB code 1qfx; Kostrewa *et al.*, 1999) and the mitochondrial NAD malic enzyme (mNAD-ME; PDB code 1qr6; Xu *et al.*, 1999), together with the tetragonal proteins vanillyl-alcohol oxidase (VAO; PDB 1vao; Mattevi *et al.*, 1997) and the mitochondrial creatine kinase (CK; PDB code 1crk; Fritz-Wolf *et al.*, 1996).

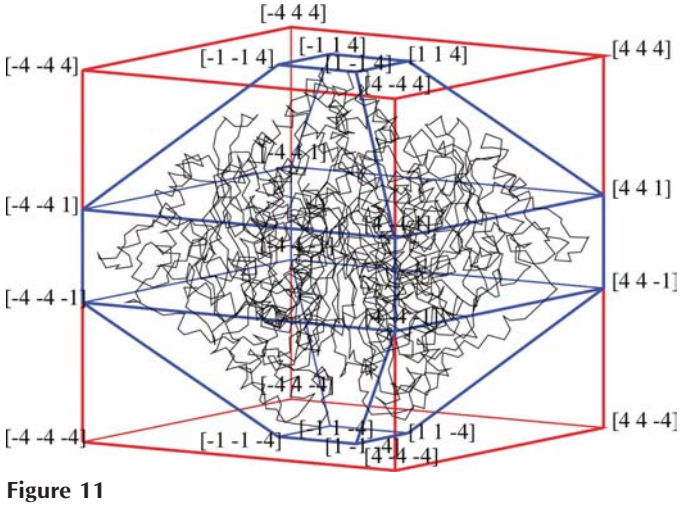

Figure 11
The same *A. niger* acid phosphatase as in Fig. 10 is shown in a perspective view. The cubic indices of the cube and of the inscribed pyramidal envelope are indicated.

In the present case, there are two types of symmetry-adapted bases: the isometric case with axial ratio $c{:}a = 1$, which in fact is cubic, and the case with ratio $c{:}a = 1/3^{1/2}$. The lattice generated by a tetragonal basis with these axial ratios apparently has a larger symmetry then the generic tetragonal lattice. This is trivial for the cubic lattice, which belongs to another Bravais class. The crystallographic investigation of lattices with a rational axial-ratio-squared (integral lattices) is in progress (Janner, 2004*b*).

4.1. Tetragonal isometric form lattice $c{:}a = 1$ (cubic)

The *A. niger* acid phosphatase, the creatine kinase octamer and the vanillyl-alcohol oxidase octamer have molecular

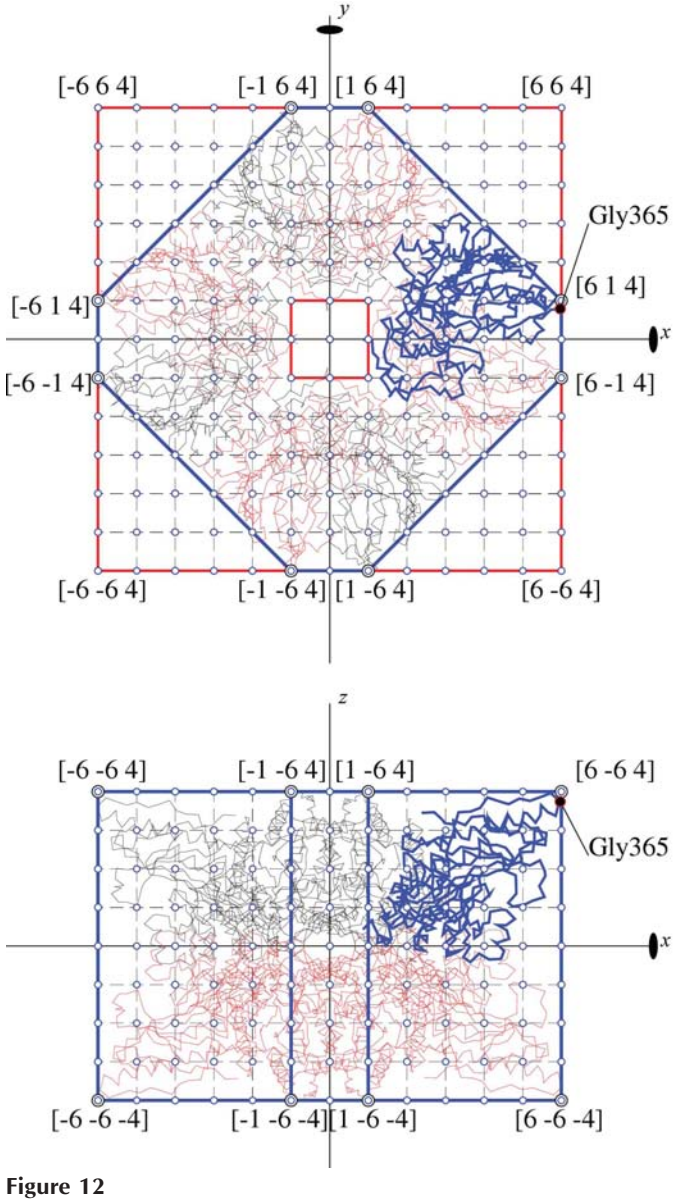

Figure 12
The 422 octamer of the mitochondrial creatine kinase (CK) is shown together with the cubic form lattice, which leads to vertices with integral indices. The maximal width of the octamer and its height are in the ratio 3:2.

forms indexed according to the points of a cubic lattice. The envelope and/or the channel need not to be a cube.

4.1.1. *A. niger* acid phosphatase (AnigAP). This protein has been considered, despite the fact that it does not have a channel of appreciable size, because it illustrates nicely how the molecular morphology of a tetramer with 222 point-group symmetry (Kostrewa *et al.*, 1999; PDB code 1qfx) reveals an unexpected underlying cubic molecular form lattice. The envelope is inscribed in a cube with an edge length of 85 Å (indicated as approximatively 80 Å in Kostrewa *et al.*, 1999). The refined envelope is a square pyramid with point-group symmetry 422, truncated in such a way that the vertices are at points of a cubic lattice with parameter a = 10.625 Å, one eighth of the edge of the cube indicated, which has vertices at 444 and cubic transformed vertices (Fig. 10). A set of representative cubic indices of the bipyramid is given by 114 and 441. The remaining ones are related to these two by the 222 symmetry (Fig. 11).

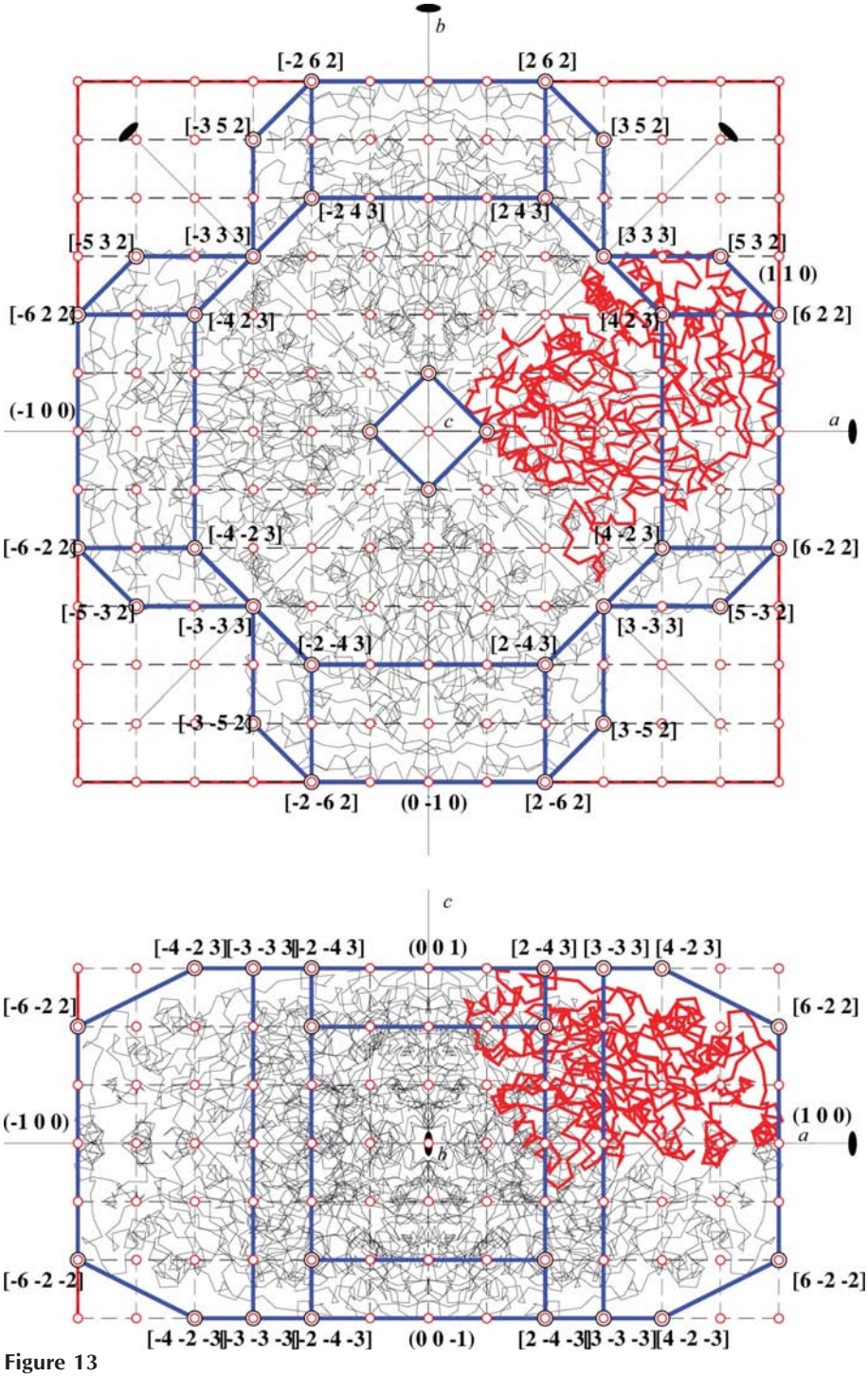

Figure 13
The tetragonal enclosing form of the tetragonal vanillyl-alcohol oxidase octamer (VAO) is shown in a view along the direction of the channel and perpendicular to it. The vertices are at points of a cubic lattice (indicated by dashed lines) labelled by their indices $[n_1, n_2, n_3]$. The indices $(h_1h_2h_3)$ of a number of faces are also given. The overall width of the envelope is twice its height.

4.1.2. Mitochondrial creatine kinase (CK). The octameric mitochondrial creatine kinase has a 42 point-group symmetry (Fritz-Wolf *et al.*, 1996; PDB code 1crk). It is a sandwich of two interpenetrating tetramers (formed by successive dimerization of the monomer) with point-group symmetry 4.

The octamer (considered already in §2) is shown in Fig. 12 in a view along and perpendicular to the fourfold axis (chosen in the z direction). The enclosing form has vertices at points of a cubic lattices with lattice parameter a = 11.45 Å. The height of the octamer is eight times the parameter a.

As already discussed in §2, the envelope of the octamer appears in the axial view as an intersection of two squares, each in one of the two orientations allowed by the point-group symmetry. Two vertices have cubic indices 614 and 164, respectively. The remaining 14 vertices follow by applying the symmetry operations of 42. In a similar way, the vertices of the channel can be obtained from the vertex with the indices 114.

The residues Gly365 and Thr1, which have an extremal radial distance from the rotational axis, are located at the lateral boundaries of the envelope and of the channel, respectively (Figs. 3 and 12).

4.1.3. Vanillyl-alcohol oxidase octamer (VAO). This protein has a 42 point-group symmetry (Mattevi *et al.*, 1997; PDB code 1vao). The enclosing forms of the octamer are shown in a view along and perpendicular to the tetragonal z axis (Fig. 13). Dashed lines indicate the underlying cubic lattice with empty circles for the lattice points. The form of this channel is a square

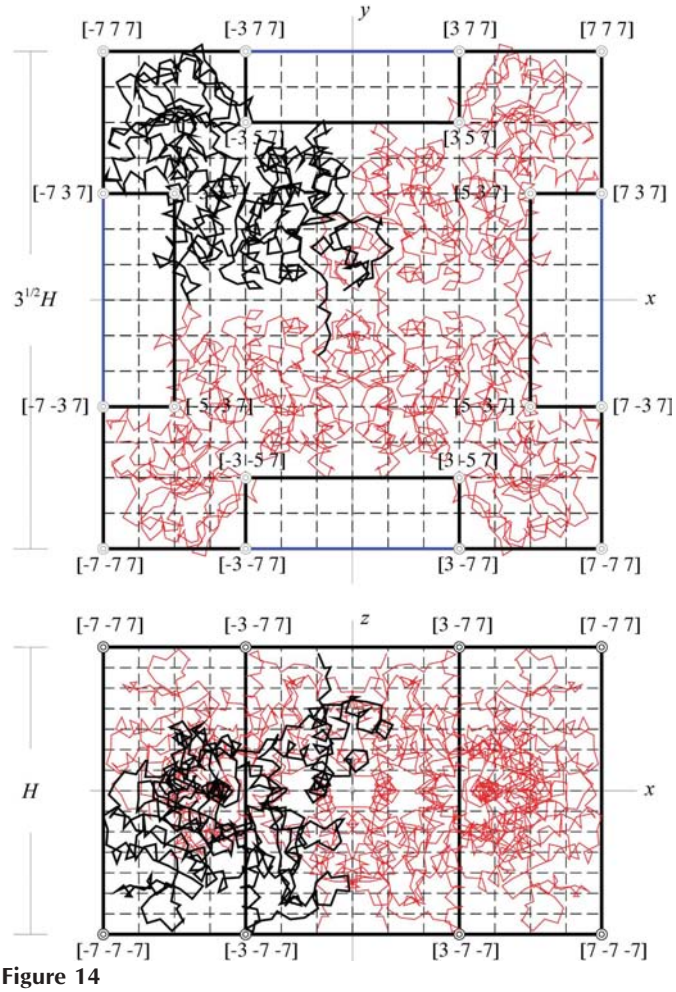

Figure 14
The orthorhombic mitochondrial NAD malic enzyme (mNAD-ME) tetramer has a tetragonal square envelope, with an edge length which is a factor $3^{1/2}$ larger than the height. The tetragonal form lattice (indicated by dashed lines) has the same axial ratio as the envelope.

prism with height 6*a* and radius *a*, the cubic lattice parameter. The form of the envelope can be refined from a starting square prism 6*a* high and 12*a* large. A complex polyhedral form is then obtained with vertices marked in Fig. 13 by double circles and with the coordinates given by corresponding sets of indices $[n_1n_2n_3]$.

4.2. Tetragonal form lattice with axial ratio c:*a* = $1/3^{1/2}$

4.2.1. Mitochondrial NAD malic enzyme (mNAD-ME). Not all tetragonal molecular form lattices observed in proteins are isometric, as shown by the example of mNAD-ME, which has a 222 point-group symmetry and a negligible central channel (Xu *et al.*, 1999).

The global envelope is a prism with as a basis a square of edge length A = 114 Å and height $H = A/3^{1/2}$ as shown in Fig. 14. In Xu *et al.* (1999) (PDB code 1qr6) the dimensions of the tetramer are specified as approximatively 110 × 110 × 55 Å. A refinement of this envelope is possible by assuming that the molecular form lattice with the axial ratio $c{:}a = 1/3^{1/2}$ is scaled from the prismatic envelope by a factor of 14, as indicated by dashed lines. The encapsulation within the refined boundaries (in bold lines) is poorer than in the tetragonal square envelope.

5. Final remark

Considerations of the possible biological implications of the morphological properties observed and on their challenging character can be found at the end of part II (Janner, 2005*a*).

Thanks are expressed to R. de Gelder, C. Hilbers and B. Souvignier for suggesting improvements, and to A. Fasolino, G. Vriend and R. Hooft for stimulating discussions

References

Belrhali, H., Nollert, P., Royant, A., Menzel, C., Rosenbusch, J. P., Landau, E. M. & Pebay-Peyroula, E. (1999). *Structure*, **7**, 909–917.
Bentley, W. A. & Humphreys, W. J. (1931). *Snow Crystals.* New York: McGraw–Hill (1962, Dover).
Chang, W., Jiang, T., Wan, Z., Zhang, J., Yang, Z. & Liang, D. (1996). *J. Mol. Biol.* **262**, 721–731.
Cowan, S. W. (1993). *Curr. Opin. Struct. Biol.* **3**, 501–507.
Edman, K., Nollert, P., Royant, A., Belrhali, H., Pebay-Peyroula, E., Hajdu, J., Neutze, R. & Landau, E. M. (1999). *Nature (London)*, **401**, 822–826.
Fritz-Wolf, K., Schnyder, T., Wallimann, T. & Kabsch, W. (1996). *Nature (London)*, **381**, 341–345.
Gelder, R. de & Janner, A. (2004). *Acta Cryst.* A**60**, s218.
Kostrewa, D., Wyss, M., D'Arcy, A. & van Loon, A. P. G. M. (1999). *J. Mol. Biol.* **288**, 965–974.
Janner, A. (2001). *Cryst. Eng.* **4**, 119–129.
Janner, A. (2002*a*). *Struct. Chem.* **13**, 279–289.
Janner, A. (2002*b*). *Z. Kristallogr.* **217**, 408–414.
Janner, A. (2002*c*). *Z. Kristallogr.* **217**, 325–326.
Janner, A. (2002*d*). *Acta Cryst.* A**58**, 334–345.
Janner, A. (2003*a*). *Proteins Struct. Funct. Genet.* **51**, 126–136.
Janner, A. (2003*b*). *Acta Cryst.* D**59**, 783–794.
Janner, A. (2003*c*). *Acta Cryst.* D**59**, 795–808.
Janner, A. (2004*a*). *Acta Cryst.*, A**60**, 198–200.
Janner, A. (2004*b*). *Acta Cryst.*, A**60**, 611–620.
Janner, A. (2005*a*). *Acta Cryst.* D**61**, 256–268.
Janner, A. (2005*b*). *Acta Cryst.* D**61**, 269–277.
Landau, E. M. & Rosenbusch, J. P. (1996). *Proc. Natl Acad. Sci. USA*, **93**, 14532–14535.
Mattevi, A., Fraaije, M. W., Mozzarelli, A., Olivi, L., Coda, A. & van Berkel, W. J. H. (1997). *Structure*, **5**, 907–920.
Tomchick, D. R., Turner, R. J., Switzer, R. L. & Smith, J. L. (1998). *Structure*, **6**, 337–350.
Xu, Y., Bhargava, G., Wu, H., Loeber, G. & Tong, L. (1999). *Structure*, **7**, 877–889.